

Pool boiling heat transfer of Novec 649 on sandblasted surfaces

Chiara Falsetti ^{a,1}, Jason Chetwynd-Chatwin ^b, Edmond J. Walsh ^{a,*}

^a Thermofluids Institute, Department of Engineering Science, University of Oxford, Oxford, UK

^b Rolls-Royce plc, Bristol, UK

ARTICLE INFO

Keywords:

Pool boiling

Heat transfer coefficient

Surface enhancement

Critical heat flux

ABSTRACT

Pool boiling represents a potentially efficient mechanism for thermal management of power electronic components. The present study investigates pool boiling heat transfer using Novec 649 on copper substrates with varying surfaces. Sandblasting, which is a relatively simple surface modification technique, has been used to obtain different copper surface roughness levels ranging from 0.1 μm to 9 μm arithmetic mean surface roughness values. The effects of surface modifications and orientation on boiling heat transfer coefficient (HTC), and critical heat flux (CHF), of Novec 649 have been experimentally investigated by performing pool boiling experiments at atmospheric pressure and saturation pool temperature. The experimental results showed that the size and orientation of the boiling surface do not have a significant impact on the CHF, whilst the HTC improves in the nucleate boiling regime with vertical orientation. In addition, for the range of surface roughness investigated improvements of $\sim 3\text{X}$ and $\sim 1.5\text{X}$ in HTC and CHF, respectively, were found relative to the original smooth surface. The HTC in the film boiling regime relative to the nucleate boiling regime was also quantified and found to be $\sim 20\text{X}$ for our geometries.

1. Introduction

Boiling heat transfer has been widely investigated and researched in a broad range of applications such as high-power electronics [1–5], IT equipment, nuclear reactors [6], and batteries [7]. Boiling heat transfer is a prominent method to obtain some of the highest possible heat fluxes of any cooling mechanism [8,9]. Among different two-phase cooling methods, direct immersion cooling has the additional advantage of removing thermal interface materials (TIMs) and thus reducing the overall thermal resistance and packaging constraints [10]. This is especially important for high heat flux devices where the TIM is a significant portion of the thermal resistance from chip to ambient. It is therefore of high interest for a wide range of cooling applications. In order to investigate this potential the present study focuses on the heat transfer in pool boiling, where the liquid near the heated surface is driven by both natural convection and by the mixing induced by bubble nucleation and departure, with different surfaces. The CHF is the limit of operation in boiling heat transfer, as higher heat fluxes result in a vapor layer forming on, and insulating, the surface resulting in a rapid surface temperature rise and leading to system failure for most electronics cooling applications. Therefore, CHF is an important design limitation

that needs to be considered.

Many research studies focused on increasing both HTC and the CHF in boiling heat transfer by focussing on varying surface augmentation to enhance fluid-surface interaction, as described in recent reviews [11, 12]. Examples of surface augmentation include modifying roughness to increase the number of active nucleation sites [13], creating regions with different wettability [14] and surface texture with microstructure [15,16]. A simpler approach has been the use of sandblasting to augment surfaces in a cost-effective way [13,15].

The effect of surface roughness on pool boiling with FC-77 fluid on aluminum surfaces was investigated by Jones et al. [17]. Their results showed that the maximum HTC and CHF increased up to 210 % and 50 %, respectively, with roughness range of R_a 0.027 μm to 10 μm . Although the trends were the same, they noted that FC-77 showed a greater variation on the HTC due to surface roughness when compared with water. Song et al. [13] investigated the use of silicon sandblasted surfaces for the enhancement of pool boiling heat transfer using deionised water. Their R_a range was between 0.1 μm and 8 μm with heat fluxes up to 200 W/cm^2 . The results showed improvements of HTC and CHF of up to $\sim 4\text{X}$ and 2X respectively when compared to a smooth silicon surface. The general trend obtained shows an increase of the HTC and CHF values with increasing surface roughness with the primary

* Corresponding author.

E-mail address: edmond.walsh@eng.ox.ac.uk (E.J. Walsh).

¹ Currently at Propulsion and Power, Delft University of Technology, Delft, The Netherlands

Nomenclature

C_p	specific heat, J/kgK
D_b	bubble departure diameter, m
CHF	critical heat flux, W/cm ²
C_{sf}	constant in Rohsenow
g	gravity m/s ²
GWP	global warming potential
HTC	heat transfer coefficient, W/m ² K
h_{fg}	latent heat of vaporization, J/kg
k	thermal conductivity, W/mK, molecular weight, g/mol
p	pressure, bar
Pr	Prandtl number
q	heat flux, W/m ²
R_a	average surface roughness, μm
T	temperature, K
ΔT	excess temperature, K
u	velocity, m/s
x	position, m

Greek Symbols

α	thermal diffusivity, m ² /s
ρ	density kg/m ³
σ	surface tension, N/m
μ	dynamic viscosity, Pa s
ν	kinematic viscosity, m ² /s
θ	contact angle, deg

Subscripts

exp	experimental
centr	central
corr	correlation
l	liquid
r	reduced
sat	saturation
v	vapor
w	wall

reason being noted as a higher number of nucleation sites. In addition, the authors suggested that capillary wicking may increase the bubble departure frequency by increasing evaporation of the thin layer of liquid near the heated surface.

Nucleate boiling heat transfer experiments with Novec 649 and a 0.001 inches nickel wire at atmospheric pressure have been conducted by Buongiorno et al. [18]. The study showed that the Novec 649 could be used as an alternative to FC-72 with similar results obtained. The experimental CHF agreed well with the Zuber correlation for small cylinders $\sim 20 \text{ W/cm}^2$.

Pool boiling of Novec 649 was also investigated by Kaniowsky [19], who compared smooth copper samples with microchannels ones (channel width of 300 μm , and height of 200–300–400 μm). The mean surface roughness was 0.122 μm . The excess temperature for boiling initiation was 10.5 K, and the CHF $\sim 11 \text{ W/cm}^2$ for the smooth sample. Their best heat transfer results were obtained with channel height of 400 μm , with an increase in the HTC of 14X compared to the smooth sample.

The study of Cao et al. [20] investigated pool boiling of Novec 649 and compared smooth copper surfaces with microparticle- and nanoparticle-coated ones. The structured surfaces showed an enhancement of both the HTC and CHF. The HTC increased from 4.5 kW/m²K for the smooth surface to 21.1 kW/m²K for the best structured one, and the CHF increased from 17W/cm² to 22.64W/cm².

Može et al. [14] tested functionalized copper surfaces for Novec 649 boiling heat transfer. The onset of boiling (ONB) for the smooth surface was 17–20 K, while it reduces to 10–12 K for the structured surfaces. The highest HTC increase within this comparison was recorded on the hydrophobized surface (13 kW/m²K at 12W/cm²), representing an enhancement of 54 % compared with the untreated surface. The results also indicate that virtually no enhancement of the HTC was achieved at high heat fluxes (close to the CHF), with degradation observed in some cases. The experimental CHF for the untreated and best treated surfaces was 20 W/cm² and 24W/cm², respectively. They did however observe a degradation of boiling performance and chemistry and morphology changes of the surface when using Novec 649. Indeed, large deviations between the first and the second boiling curve obtained from experiments on the same sample were observed, while this effect was not observed in water.

Ghaffari et al. [21] experimentally investigated Novec 649 boiling heat transfer on a copper surface. The boiling initiated at a wall superheat temperature of 12 °C and the measured maximum HTC of 8kW/m²K with CHF of 17.4 W/cm². They measured the performance of plates with different thickness and a larger surface area than the heater.

The non uniform heat transfer conditions caused a decrease in the CHF of 50 % compared to the reference case. In order to improve lateral spreading and obtain the same CHF with the reference case, the thickness of the plate was increased from 1 mm to 5 mm.

An experimental study comparing sandblasted and sandpapered surfaces with HFE-7200 was performed by Shamsaiee et al. [22]. The sandblasted surfaces showed an earlier onset of boiling compared to the sandpapered ones with same average roughness, and a larger increase in heat transfer of $\sim 2\text{X}$ versus $\sim 1.7\text{X}$. The profilometry results underlined a difference in cavities generated by the two different machining techniques, suggesting that sandblasting was increasing heat transfer more as a result of more densely packed cavities.

As indicated by previous reviews [11,12], there is the need of creating larger database for dielectric refrigerants and surface treatments to provide optimal design guidelines for surface conditioning and higher-performance cooling systems. Studies have been conducted with water and fluorocarbons fluids on sandblasted surfaces, but no studies are available on pool boiling of Novec 649 with sandblasted surfaces and different orientations. The few studies investigating pool boiling of Novec 649 used micro-structured or coated surfaces only. This study contributes to filling this gap by experimentally characterising the thermal performance of Novec 649 with sandblasted surfaces. Novec 649 has a very low environmental impact (GWP = 1 and ODP = 0), it is not flammable or toxic and is non-electrically conductive and it is therefore of interest for practical use in electronics thermal management.

In this study, the effects of different surface roughness and of surface orientation on pool boiling heat transfer of Novec 649 are investigated. The arithmetic mean surface roughness values, R_a , range from 0.1 μm to 9 μm . The increase in surface roughness obtained by sandblasting has a positive impact on heat transfer, in agreement with previous studies with other dielectrics. In particular, the experimental results indicate an increase of $\sim 3\text{X}$ and $\sim 1.5\text{X}$ in the HTC and CHF, respectively.

2. Experimental set up

2.1. Pool boiling facility and test section

The pool boiling facility consists of a pressure chamber made of a polycarbonate cylinder of 150 mm inner diameter and 184 mm height, with a stainless steel base and an aluminum lid that can operate up to 4 bar, see Fig. 1(a and b).

A silicon O-ring around the perimeter and four stainless steel star

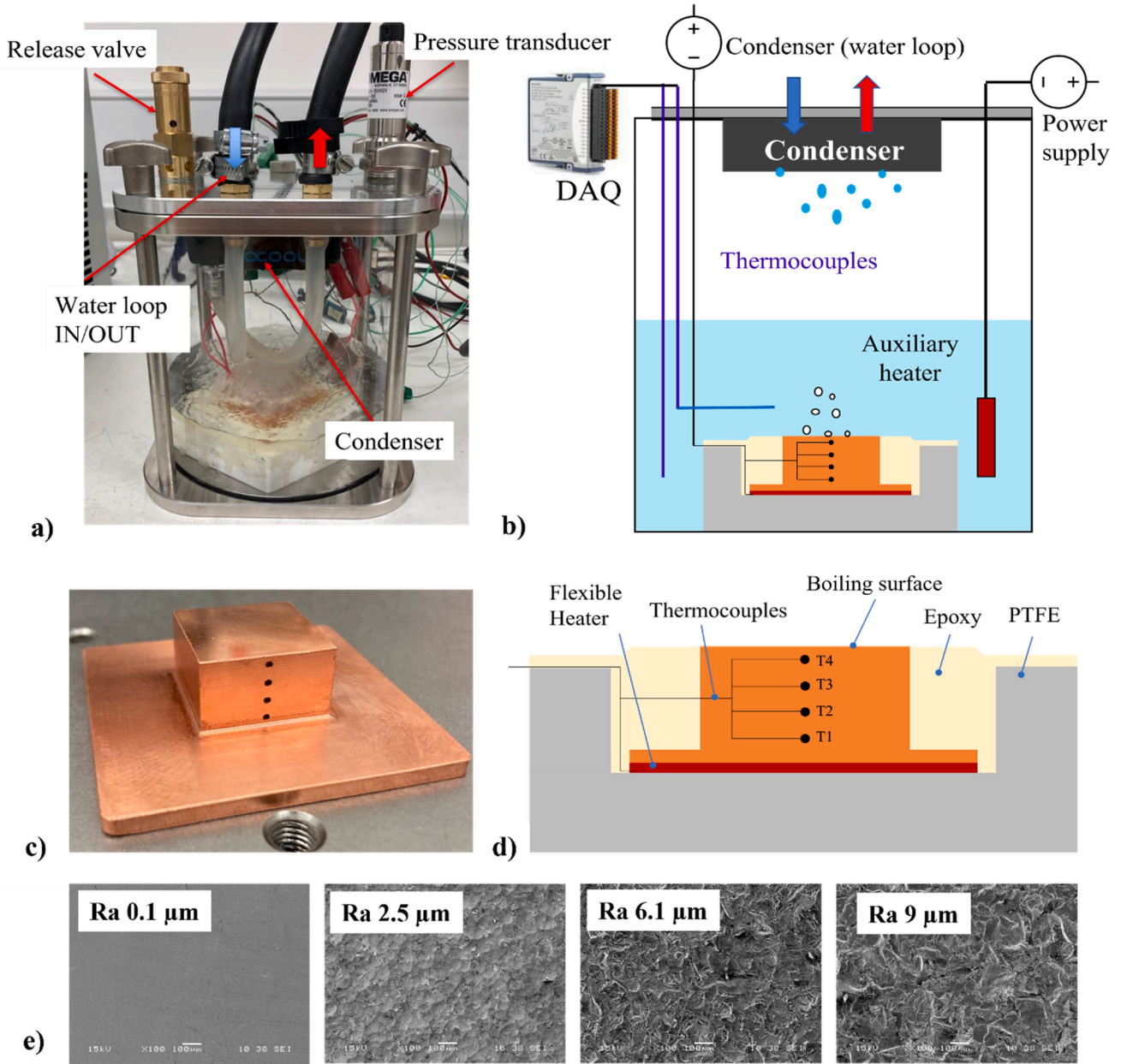


Fig. 1. (a) Photograph and (b) schematic of the pool boiling setup: pressure vessel with embedded instrumentation and test section merged in the pool. (c) Copper smooth test section (SR1), and (d) Cross-section of the test section assembly. (e) SEM Images of the sandblasted and smooth surfaces. Scale 100 μm .

grips are used to seal the vessel. A safety relief valve and an absolute pressure transducer, to measure the pressure inside the vessel, are installed on the lid. Two K-type thermocouples measure the liquid temperature inside the vessel, four thermocouples are installed in the copper test section. An adhesive flexible resistance heater is attached to the test section to control heat flux. An auxiliary heater is submerged in the pool to control the pool temperature during experiments. The thermocouples and heater connection wires are going through the lid and are sealed with two-part epoxy. An Alphacool NexXos radiator, connected to a temperature controlled water loop (Lauder bath), is installed on the inside of the lid to act as the condenser, see Fig. 1. The water temperature and/or flow rate is used to control the pressure and hence saturation temperature, and hence pressure, in the pressure chamber. Experiments have been performed with Novec 649 at 1 bar, with a corresponding saturation temperature of 49 °C. Leak testing was performed by holding the chamber at pressures up to 2 bar. The utilized 3 M fluid Novec 649 has low global warming potential (GWP), and is

dielectric, non-flammable and non-toxic. Its thermophysical properties are widely available, REFPROP library, and are summarized in Table 1 at 1 bar.

The test section consists of a T-shape copper block, as depicted in the picture and schematic of Fig. 1(c and d), with a bottom plate of area 51 mm x 51 mm and thickness of 5 mm, and the top boiling surface of either 35 mm x 35 mm or 20 mm x 20 mm and thickness of 12 mm. Four holes of 1 mm diameter, are machined in the test section along the vertical direction to measure the temperature and calculate the heat flux, as outlined in Section 3. The distance between each hole is 3 mm and the distance of the top hole to the boiling surface is equal to 1.5 mm. An OMEGA flexible adhesive flexible heater is attached to the bottom surface and powered by an external power supply as the heat source. The test section is housed in a PTFE support and insulated by two-part epoxy, see Fig. 1(d). The nominal samples, as the one depicted in Fig. 1(c), have a polished surface with an arithmetic mean roughness, R_a of 0.13 μm and corresponding root-mean square roughness, R_q , of 0.18 μm . These are

Table 1

Thermophysical properties of Novec 649 at 1 bar, saturation temperature 49 °C.

	$\rho_l \left[\frac{\text{kg}}{\text{m}^3} \right]$	$\rho_v \left[\frac{\text{kg}}{\text{m}^3} \right]$	$\sigma \left[\frac{\text{N}}{\text{m}} \right]$	$h_{lv} \left[\frac{\text{J}}{\text{kg}} \right]$	$\mu_l [\text{Pa} \cdot \text{s}]$	$Pr_l [-]$	$M [\text{g/mol}]$
Novec 649	1.5254e + 03	12.9806	0.0089	8.7806e + 04	4.8494e-04	10.09	316

referred as a “smooth” sample, labeled SR1, and provide a baseline for comparison with the modified surfaces.

For the present study, the boiling surface has been modified by sandblasting to investigate its impact on heat transfer enhancement. In addition to the smooth sample SR1, three different samples with arithmetic mean roughness values of R_a of 2.5 μm , 6.1 μm and 9 μm and corresponding root-mean-square roughness, R_q , of 3.3 μm , 7.9 μm , and 12 μm , have been obtained using different medium particle sizes. The samples are labeled SR2, SR3 and SR4 with increasing roughness, details are given in see Table 2. The roughness was measured by an optical profiler, μSurf Nanofocus.

The sandblast mediums used were Honite soda-lime glass bead (from 106 μm to 212 μm), and Saftigrit Brown, brown alumina manufactured by reduction melting from high grade bauxite (54 μm). The sandblasting process was done by a dry blast system at 40 psi blast pressure for 3 min approximately, at a distance of 100 mm from the surface and impingement angle of 70°. SEM images of the smooth and sandblasted surfaces are shown in Fig. 1e. From the SEM images, where ridges and cavities across the surface can be seen.

3. Data reduction and experimental procedure

3.1. Data reduction and uncertainty

The data reduction procedure to calculate the heat flux and HTC is presented in this section.

The heat flux is calculated by Fourier’s law assuming 1D conduction in the copper test sample. The copper sample is insulated on all sides except the top surface, and assumes that the heat flux can be evaluated using:

$$\dot{q} = -k \frac{dT}{dx} \quad (1)$$

The spatial temperature gradient, $\frac{dT}{dx}$, is calculated by a linear interpolation of the four thermocouple measurements, confirmed to an accuracy of 0.2 °C. The distance between two neighbouring thermocouples is dx . The thermal conductivity of the copper sample is $k = 390 \frac{\text{W}}{\text{mK}}$. An example of the linearity of the thermocouples installed in a copper sample during two different tests is shown in Fig. 2.

The temperature of the boiling surface, T_w , if found by extending the liner gradient to the surface as:

$$T_w = T_4 - \frac{\dot{q} \cdot \Delta x}{k} \quad (2)$$

The level of superheat, also called excess temperature, is calculated as the difference between the surface temperature and the saturation temperature of the cooling liquid $\Delta T = T_w - T_{sat}$. The pool was at saturation conditions at 1 bar pressure as confirmed by the saturation temperature T_{sat} obtained as the average of the measurements of the two thermocouples submerged in the liquid pool. The HTC is calculated using:

Table 2

Test section roughness and sandblasting medium.

Sample	$R_a [\mu\text{m}]$	$R_q [\mu\text{m}]$	Blasting particle size [μm]
SR1	0.13	0.18	54
SR2	2.5	3.3	106
SR3	6.1	7.9	150
SR4	9	12	212

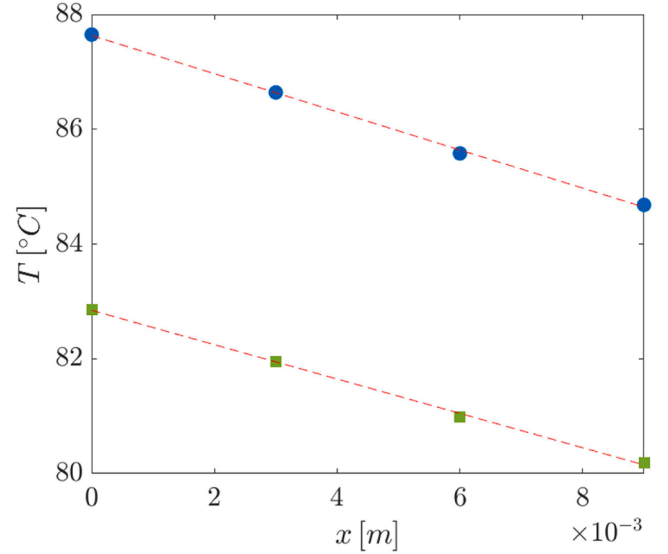


Fig. 2. Example of linear fitting to calculate the 1-D heat flux through the copper surface.

$$HTC = \frac{\dot{q}}{T_w - T_{sat}} \quad (3)$$

The uncertainties associated with the wall temperature, heat flux and HTC are estimated by using the established propagation method of Kline and McClintock [23]. The uncertainty of each variable is given in Table 3.

Before performing the pool boiling experiments, the liquid was degassed for 30–40 min using the electrical heaters and venting to atmosphere. During experiments the vent is sealed and temperatures recorded from the thermocouples after steady-state is reached, steady-state defined as less than 0.2 °C variation for a period of 4 min.

3.2. Repeatability

Pool boiling experiments were repeated with the same test section and surface finish on different days to ensure repeatability. The samples were not altered between runs. The repeatability tests have been done

Table 3

Uncertainty values of parameters of interest.

Variable	Instrument	Uncertainty
Liquid and copper Temperature, T_{sat}	K-Type thermocouple	0.2 °C
$T_1 - 4$		
Vapor pressure, p_v	Absolute pressure transducer	0.08 % $\pm 0.2 \text{ kPa}$
Thermal conductivity, k	Manufacturer	1 % $3.9 \frac{\text{W}}{\text{K} \cdot \text{m}}$
Positioning, x	Measured	0.2 mm
Heat flux, q	Calculated (Eq. (1))	[4.8–11.4] %
Wall Temperature, T_w	Calculated (Eq. (2))	0.34 °C
Superheat, $T_w - T_{sat}$	K-Type thermocouple	0.39 °C
HTC	Calculated (Eq. (3))	[5–12.1] %

for the smooth (SR1) and the sandblasted samples (SR 2-3-4). Boiling curves of the four samples obtained from two different days are presented in Fig. 3. In general the plot shows good repeatability within the maximum uncertainty of the heat flux (11.4 %), indicated by the error bars in the plot.

The repeatability for the highest surface roughness sample (SR4) has the largest deviation, see Fig. 3(d). A maximum temperature difference of 10.5 K has been observed for the same heat flux of 18.5 W/cm^2 . The deterioration of heat transfer is indicated by the shift of the boiling curves towards higher excess temperatures, and it is more severe with higher surface roughness. These results may suggest that Novec 649 or/and the bubbles activity impact the surface condition and, therefore, the boiling heat transfer. Measurement of roughness post experiment showed a reduction of $\sim 15\%$ compared to the same sample before experiments. Further research is needed to investigate this effect and understand the origins better.

However, similar observations are reported by Moze et al. [14], who found a difference in the wall superheat up to 20 K for a given heat flux when using Novec 649. Aging effects have been also found with micro-porous coatings and HFE-7200 cooling fluid by Wu et al. [24]. When using coatings, the authors suggested to perform annealing to improve structural durability. No deterioration has been reported in the literature when using water, suggesting that the reason behind it might be related to the fluid itself rather than bubbles activity.

Further repeatability (aging) tests were undertaken on different days for specimens SR1-2-3-4, and the maximum excess temperature was found to be within 10.5 K for the sandblasted surface SR4. A difference was found between first and subsequent tests at the higher heat fluxes, hence the data presented in the results section are those averaged after multiple runs.

4. Experimental results and discussion

In this section the experimental results are outlined and discussed. The results are presented in terms of boiling curves, i.e., heat flux (q) as a function of wall superheat, HTC and CHF.

4.1. Smooth sample heat transfer and size effect

The boiling curve of the two different sized test vehicles, $20 \times 20 \text{ mm}^2$ and $35 \times 35 \text{ mm}^2$, having the same surface finish (SR1) are shown in Fig. 4. The onset of boiling (ONB) occurs at the same wall excess temperature of $\Delta T \sim 20 \text{ K}$ for both the samples, and the HTCs are closely aligned up to $\sim 10 \text{ W/cm}^2$. The CHF limits are measured to within $\sim 10\%$ with the smaller test vehicle having the higher CHF which agrees with most correlations showing that CHF is higher for smaller geometrically similar heated surfaces [25]. The experimental data are compared to two well-known correlations for pool boiling heat transfer

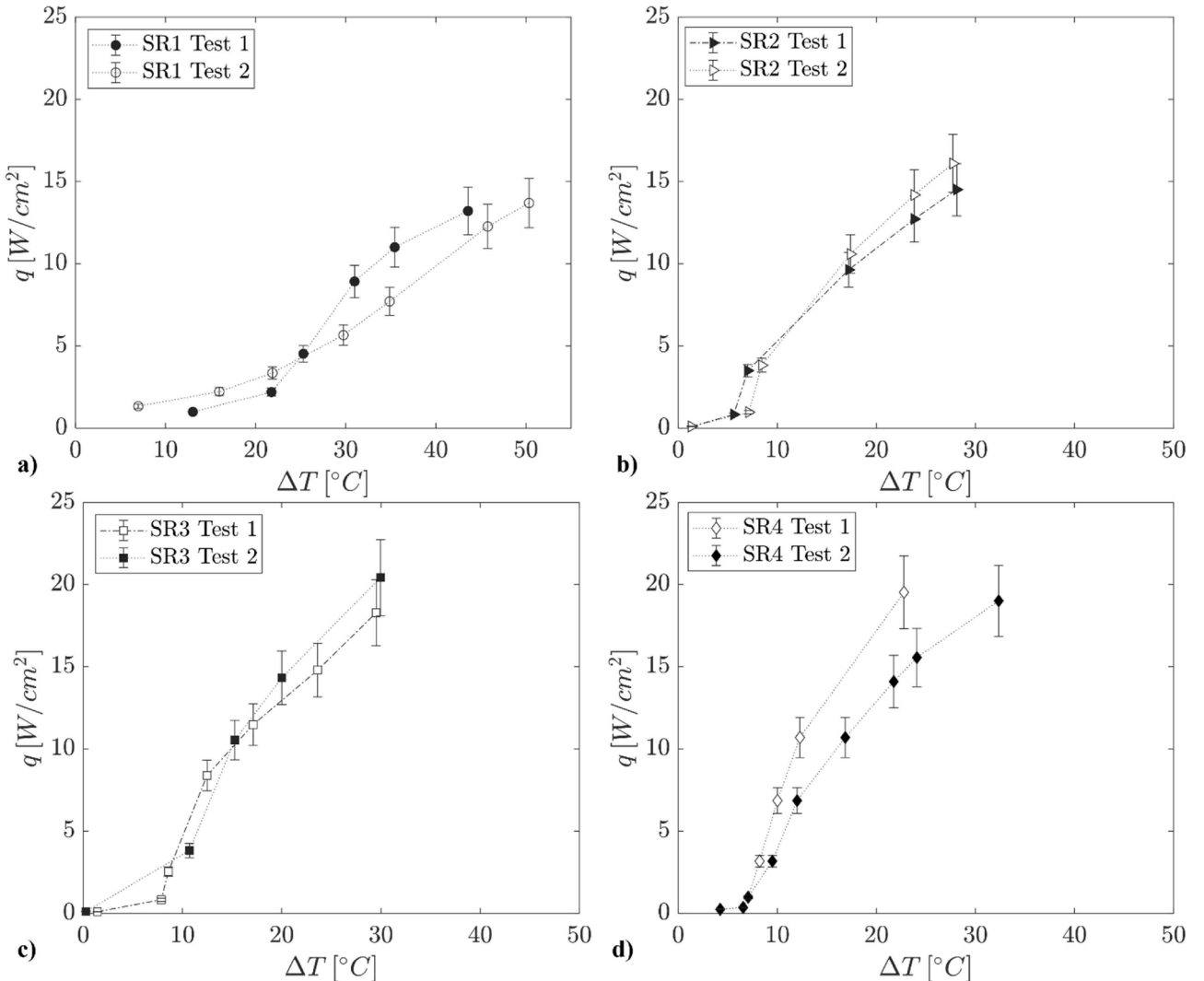


Fig. 3. Repeatability of pool boiling experiments for (a) SR1, (b) SR2, (c) SR3, (d) SR4.

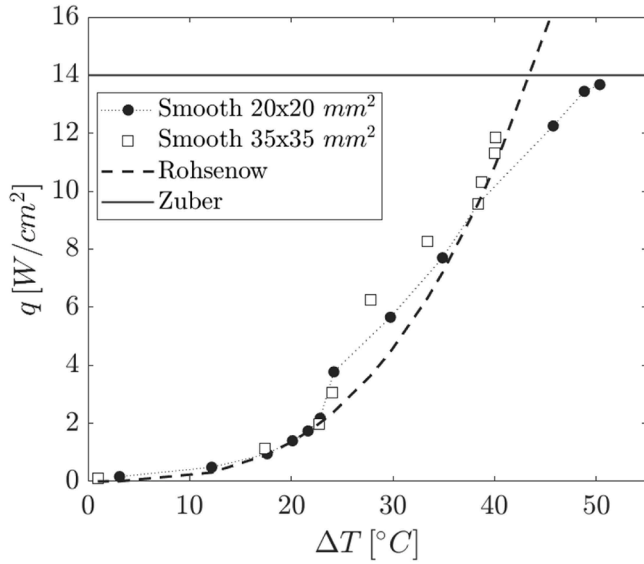


Fig. 4. Boiling curves of smooth test sections (SR1) with different boiling surface dimensions. Comparison with Rohsenow's correlation and Zuber's CHF predicted value. The CHF value is included in the plot.

using the thermophysical properties at saturated conditions indicated in Table 1. The Rohsenow's correlation [26] to predict the heat flux is given as:

$$q' = \mu_l h_{fg} \left[\frac{g(\rho_l - \rho_v)}{\sigma} \right]^{0.5} \left[\frac{c_p(T_w - T_{sat})}{C_{sf} h_{fg} Pr_l^n} \right]^3 \quad (4)$$

The coefficient C_{sf} and the exponent of the Prandtl number, n , depend on the condition and material of the boiling surface and the fluid-surface combination. Rohsenow suggested a value of $n = 1$ for water, and $n = 1.7$ for other fluids [26], therefore the latter is used in this study. Typical values of C_{sf} found in experimental pool boiling studies using refrigerants and copper surfaces range from ~ 0.005 to ~ 0.015 . In this study a value of C_{sf} of 0.008 was chosen to best fit the current data of the smooth sample (SR1). To estimate the prediction accuracy of the correlation, the mean absolute error (MAE) has been calculated, defined as:

$$MAE = \frac{1}{N} \sum_{i=1}^N \frac{|htc_{corr,i} - htc_{exp,i}|}{htc_{exp,i}} \quad (5)$$

Rohsenow's correlation predicts the experimental results with an MAE of 23.8 % considering both surfaces.

The experimental CHF limit is compared to Zuber [27] prediction, indicated by a horizontal solid line in Fig. 4, calculated using:

$$CHF = \frac{\pi}{24} h_{lv} (\sigma g \rho_v^2 (\rho_l - \rho_v))^{1/4} \quad (6)$$

At 1 bar the correlation predicts a CHF of 14 W/cm² for Novec 649, which agrees well with the experimental value of ~ 13.6 W/cm² found in this study.

The CHF calculated using Zuber's correlation [27] can be used to scale between different fluids for a given fluid-surface interaction as it based on fluid-properties only. For example, when considering water thermophysical properties at ambient pressure, the predicted value of CHF is 108 W/cm², which is almost 8 times larger than for Novec 649.

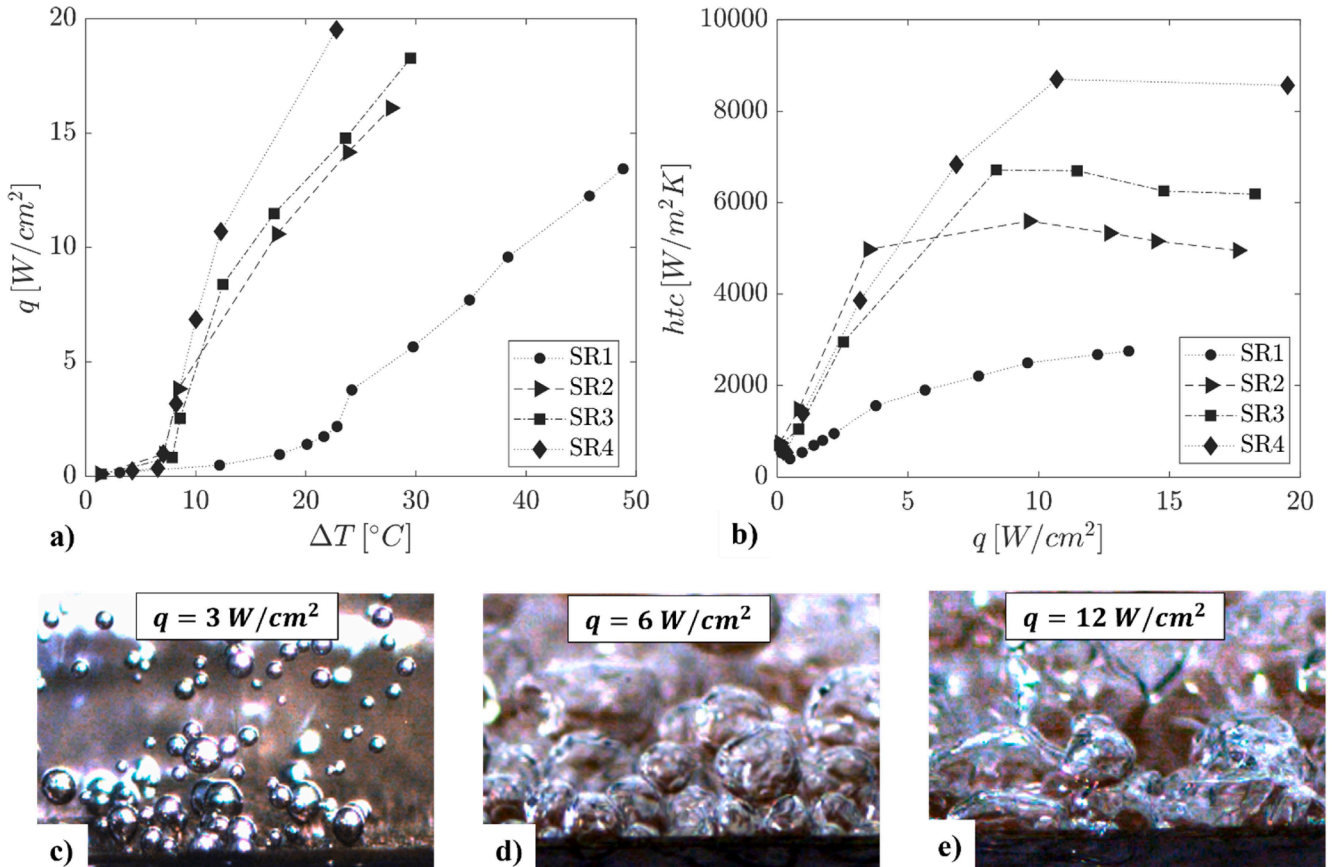


Fig. 5. (a) Boiling curves and (b) HTC values of different surface roughness test vehicles. (c-e) Pictures of the isolated and coalesced bubble regimes at different heat fluxes.

4.2. Surface roughness effects on heat transfer

The boiling curves and the HTC as a function of heat flux for the smooth (SR1) and sandblasted samples (SR2-SR3-SR4) are shown in Fig. 5(a and b). Compared to the smooth surface, the sandblasted samples demonstrate the onset of boiling at an increasingly lower excess temperatures (from $\sim 20^\circ\text{C}$ to $\sim 7^\circ\text{C}$) and improved HTC with increasing surface roughness. The CHF limit is also enhanced by increasing surface roughness: CHF of 17.6 W/cm^2 , 18.9 W/cm^2 and 20 W/cm^2 (29–47 % larger than the smooth sample SR1) were found for the SR2, SR3 and SR4 samples, respectively. From an application standpoint, having an earlier ONB allows to operate at lower junction temperatures, and therefore increase the heat flux of the device for same upper temperature limit. This, together with the increase of CHF limit, allows to extend the power dissipation range of the device.

During the pool boiling experiments, it was possible to distinguish different flow regimes before CHF occurs, these are depicted in the images of Fig. 5(c–e). The images were captured with a Phantom VEO 610 at 5000 fps. After the onset of nucleation, at low heat fluxes (in the range of $\sim 1\text{--}3\text{ W/cm}^2$), distinct small diameter bubbles nucleate from the heated surface (isolated bubble regime) from the active sites, as depicted in the picture of Fig. 5(c). When increasing the heat fluxes (at a heat flux larger than 4 W/cm^2), the bubble nucleation becomes fully developed and it is no longer possible to distinguish the single bubbles (coalesced bubbles/mushrooms regime), see Fig. 5(d). The bubbles tend to merge with increasing heat flux, forming larger bubbles, see Fig. 5(e).

The results shown in Fig. 5(a and b) indicate that the HTC is enhanced for the sandblasted samples (SR2-3-4) compared to the smooth one (SR1), as the surface roughness results in an increase of bubble nucleation sites. In the full nucleation regime, when coalesced bubbles are observed at higher heat fluxes, the HTC increases with surface roughness by 55 % when comparing the maximum HTC for SR2 and SR4, see Fig. 5(a and b). It is possible to observe that the HTC increases steeply at lower heat fluxes, when the nucleation starts, and the number of nucleation sites grows. At higher heat fluxes, the HTC starts to flatten, and it decreases when the CHF limit is approached, as a result of the flattening of the boiling curve approaching CHF. The maximum values of HTC are found during the fully developed nucleate boiling regime, which represents the optimal operational point.

As the CHF is approached vapor columns and liquid slugs are formed and the wall temperature increases and hence the HTC starts to flatten, see Fig. 5(b). When the CHF condition occurs, the vapor covers the surface, and the temperature rapidly increases. In the pool boiling literature, the effect of surface roughness on boiling and the CHF limit was studied by Song et al. [13], who performed water pool boiling experiments with copper sandblasted samples having similar values of mean roughness. They obtained a CHF varying from 103.8 W/cm^2 for the polished surface to 135 W/cm^2 for the $R_a \sim 8\text{ }\mu\text{m}$. Kim et al. [28] also found a strong dependence of CHF on surface roughness for copper surfaces using water: CHF increased from 77.5 W/cm^2 for a smooth surface with $R_a = 0.041\text{ }\mu\text{m}$ to a CHF value of 162.5 W/cm^2 for a rough surface with $R_a = 2.36\text{ }\mu\text{m}$. Results from Jones et al. [17] with FC-77, which has similar properties of Novec 649, showed CHF values of 13.7 W/cm^2 for the polished surface and of 19 W/cm^2 for the $2.2\text{ }\mu\text{m}$ surface roughness surfaces, similar to the current CHF values obtained in the current experiments. Using the CHF correlation of Zuber to estimate the heat flux scaling between water and Novec 649, the CHF would be expected to be ~ 8 times larger than with Novec 649, which is consistent with the literature value for water on sandblasted surfaces.

A picture of the CHF conditions and an example of the wall temperature increase is depicted in Fig. 6 for the smooth sample (SR1). The four series are the measured temperatures of the four thermocouples installed in the copper test section, as described in Section 2. At time 0 s, the temperatures are around 90°C and the flow regime presents a strong bubble activity. In this phase, the wall temperature increases at a rate of $\sim 2^\circ\text{C/min}$ until dry-out conditions occur, as indicated by CHF in Fig. 6.

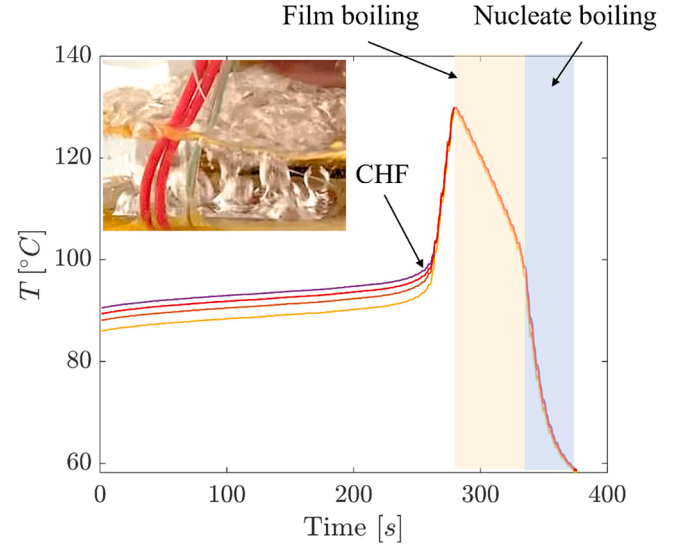


Fig. 6. Temperature evolution of the four thermocouples in the copper test vehicle (SR1) and picture during CHF conditions.

When the vapor forms a blanket on the boiling surface, the surface temperature increases rapidly $\sim 90^\circ\text{C/min}$. When the wall temperature starts rising quickly, the power is switched off, so the temperature peaks (at $T \sim 130^\circ\text{C}$ in Fig. 6) and then it starts to drop. Above CHF conditions occur, the encountered regime is film boiling, where the boiling surface is covered by a vapor layer, see inset image illustrating vapor columns emerging from vapor layer. The surface cools down, until the nucleate boiling regime re-establishes, and the regimes shown in Fig. 5(c and d) are initiated again. The film and nucleate boiling regions are indicated by the yellow and blue shaded regions respectively in Fig. 6, where it is possible to see the cooling effect of the nucleate boiling regime re-established after film-boiling. Looking at the temperature across the thermocouples in the region to the right of the figure with low heat flux, the thermocouples are within experimental uncertainty indicating an isothermal test specimen.

Considering the part of the data series after the power is turned off in Fig. 6, at the start of the shaded region when temperature starts reducing, the slope dT/dt is linearly proportional to the heat flux. For the current data this results in ~ 3.5 -fold higher dT/dt , and hence heat flux, in nucleate versus film boiling regime. However, this is the total loss rather than the heat loss due to convection on the boiling surface. To estimate the heat flux through the boiling surface the heat lost to surroundings during normal experimental conditions, i.e. heater on, is estimated. By subtracting the heat flux calculated from the thermocouple stack from the power supply input, the heat lost to surroundings away from the surface of interest was estimated at 20–25 % of the total power supplied. In the film boiling regime, the amount of heat lost through the support PTFE block can conservatively (as surface temperature will be higher) be assumed to remain at 25 %. Hence, for this experiment the ratio of heat flux through the top surface is ~ 20 times less in film boiling, compared with nucleate boiling calculated from the expression below:

$$\frac{q_{\text{film}}}{q_{\text{nucleate}}} = \frac{q_{\text{film}} - 0.25q_{\text{total}}}{q_{\text{nucleate}}} = \frac{\frac{dT}{dt}_{\text{film region}} - 0.25\frac{dT}{dt}_{\text{nucleate region}}}{0.75\frac{dT}{dt}_{\text{nucleate region}}} \quad (7)$$

A summary of the experimental results with the smooth and modified test sections is outlined in Table 4. The uncertainty of the CHF is equal to 4.8 %, which gives an absolute error of 0.65 W/cm^2 (SR1) and a maximum of 0.97 W/cm^2 (SR4). It is possible to see how the heat transfer enhancement and the CHF limit are not linearly increasing with surface roughness, but their values start to plateauing.

Table 4

Summary of the heat transfer results: CHF and maximum HTC.

Sample	CHF [W/cm ²]	Max HTC [W/m ² K]
SR1	13.6	2754
SR2	17.6	5594
SR3	18.9	6721
SR4	20	8700

4.3. Comparison with pool boiling correlations

In the last decades, many correlations have been developed to predict the pool boiling heat transfer and the effects of surface roughness for water and dielectric hydrofluorocarbons and refrigerants, but less is available for Novec 649 despite its promising environmental properties. Existing well-known nucleate pool boiling correlations, developed for copper surfaces and pressures in the same range of this study, have been selected to compare with the current experimental data. These are listed in Table 5. The correlations developed by Cooper [29], Ribatski and Jabardo [30] and Nishikawa–Fujita [31] use the reduced pressure to fit the HTC.

The correlation of Stephan [32] was developed for refrigerants and requires the knowledge of the bubble departure diameter. For this study, the capillary length scale is used as the bubble departure diameter, D_b , estimated by ratio of buoyancy to interfacial forces, as $\sqrt{\gamma/(\rho_l - \rho_v)g}$ and equal to 0.8 mm. Li et al. [33] provides a correlation which has a similar form to Rosenhow but has an prediction for the constant C value which takes into account surface roughness, contact angle and thermophysical properties of the coolant.

All the predictive correlations include a parameter or constant to account for the fluid-surface interaction, as the boiling phenomena are affected by the thermophysical properties of the fluid, the wetting characteristics of the surface and the material properties.

For the correlations which include surface roughness (R_a) the original authors proposed constants are used. However, for the Rohsenow [26] and Stephan and Abdelsalam [32] the constant was changed to best

Table 5

Pool boiling correlations including surface roughness effect.

Author	Correlation	Fluid & surface
Rohsenow [26]	$q'' = htc \cdot \Delta T_e = \mu_l h_{fg} \left[\frac{g(\rho_l - \rho_v)}{\sigma} \right]^{0.5} \left[\frac{C_p(T_w - T_{sat})}{C_{sf} h_{fg} Pr_l^n} \right]^3$	Water, Copper, stainless steel, aluminum
Ribatski and Jabardo [30]	$htc = f_p q'' p_r^{0.45} (-\log_{10} p_r)^{-0.8} R_a^{0.2} M^{-0.5}$ $m = 0.9 - 0.3 p_r^{0.3}, f_p = 100$	R11, R123, R12, R134a, R22, Copper, brass, stainless steel
Stephan and Abdelsalam [32]	$htc = K_s \frac{k_l}{D_b} \left(\frac{q D_b}{k_l T_{sat}} \right)^{0.745} \left(\frac{\rho_v}{\rho_l} \right)^{0.581} \left(\frac{\nu_l}{\alpha_l} \right)^{0.533}$ $K_s = 207$	R11 Copper
Nishikawa–Fujita [31]	$htc = K_a \frac{P_c^{0.2}}{M^{0.1} T^{0.9}} q^{0.8} \left(\frac{1 - P_r}{8 R_a} \right)^{\frac{1}{5}} \frac{P_r^{0.23}}{(1 - 0.99 P_r)^{0.9}}$	R11, R21, R113, R114, Copper
Cooper [29]	$htc = K q^{0.67} p_r^n (-\log_{10} p_r)^{-0.55} M^{-0.5}$ $n = 0.12 - 0.2(\log_{10} R_a / 0.4), K_c = 55$	Refrigerants Copper
Li et al. [33]	$htc = 518503 C_s \frac{\Delta T_e^{2.03}}{\mu_l h_{fg}} \left[\frac{g(\rho_l - \rho_v)}{\sigma} \right]^{0.5} k_l^{3.03}$ $C_s = (1 - \cos \theta)^{0.5} \gamma^{-0.04} \left[1 + \frac{5.45}{(R_a - 3.5)^2 + 2.61} \right]$	Water, ethanol, CCl4, acetone, n-hexane, R113, R141b Copper, Aluminum

fit the current data. The two-phase data only have been considered in the comparison, excluding the data before the onset of boiling and the CHF values. The comparisons are presented in Table 6 as average MAEs. As it is possible to see, the original correlation from Ribatski and Jabardo [30] predicts the data within an average MAE over the four samples of 22.8 %. The correlations from Rohsenow [26] and Stephan and Abdelsalam [32] require their constants to be fit to the data, and the average MAEs are of 41.4 % and 22.4 %, respectively. The correlation from Cooper [29] with original constant ($K_c = 55$) has a prediction error average of 91, 92.3, 95, 101 % on the SR1-2-3-4, respectively. However, tuning the constant of the surface-fluid interaction improve the prediction accuracy, as indicated in the results in Table 6. Similarly, the correlation by Nishikawa [31] with the original constant has uncertainties on predicting the current data set of 48-52-43 and 54 % for the samples SR1-2-3-4, respectively.

4.4. Vertical orientation effect

Experiments to evaluate the effect of orientation on pool boiling heat transfer have been performed. The pool boiling heat transfer has been extensively studied with horizontal-upward boiling surfaces (0°), but the study on different surface orientations has been limited to the vertical orientation (90°) as it is commonly found in immersion cooling applications.

The comparison of the boiling curves between the two orientations for the smooth (SR1) and sandblasted (SR3) test vehicles are shown in Fig. 7. The vertical orientation was only tested for two conditions, smooth and medium roughness.

For both the smooth and sandblasted samples, the boiling curves shift to the left and the HTC increases from the horizontally upwards (0°) to the vertical (90°) orientation, in agreement with previous studies [34–36].

The HTC increases in the nucleate boiling regime likely as a result of the increased buoyancy associated with the vertical orientation which results in more efficient bubble removal from the surface, see Fig. 7. Moreover, the vertical orientation seems to reduce the ONB value of ~9 K and ~3 K for the SR1 and SR3 samples, respectively, while the CHF limit remains unchanged in agreement with previous experiments [37].

At higher heat fluxes, between 8 and 13 W/cm², corresponding to the fully nucleate boiling regime, the HTC peaks and then tend to decrease due to the flattening of the boiling curve approaching CHF values, in accordance with previous studies [35]. These results indicate that the vertical orientation enhances pool boiling heat transfer with Novec 649, but does not alter the CHF. This trend is comparable to what has been observed with other fluids, including water and other dielectrics fluids.

5. Conclusions

This study experimentally investigated pool boiling heat transfer of Novec 649 on copper surfaces. Sandblasting has been used as a surface modification technique due to ease of manufacture and and cost-effectiveness. The effects of surface roughness, size and orientation of the boiling surface using Novec 649 as the heat transfer fluid have been assessed by performing experiments at ambient pressure.

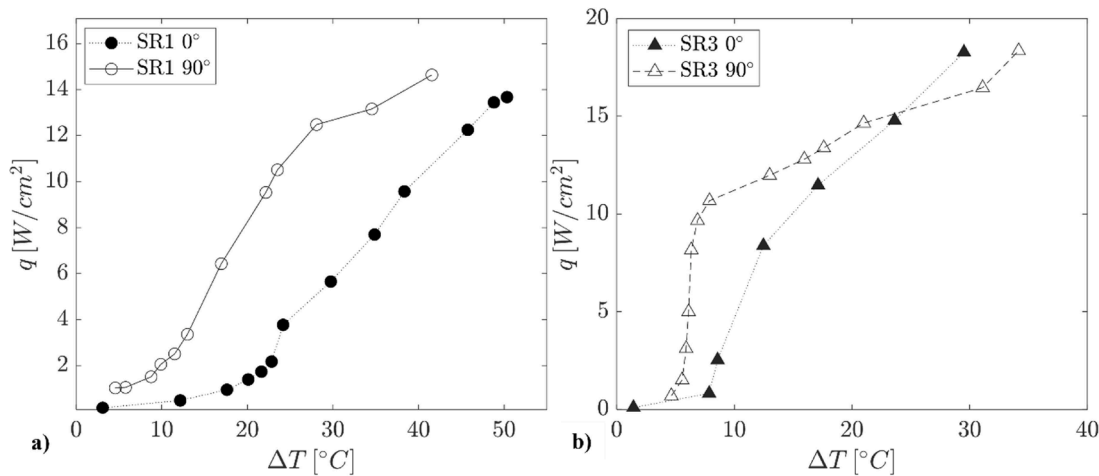
The main findings of this study are summarized below:

- 1) Increasing surface roughness by sandblasting has a positive impact on the boiling heat transfer of Novec 649, demonstrated by an increase of both the HTC and CHF limit values simultaneously. The sandblasted surfaces outperformed the smooth copper samples over the entire boiling curve. However, a degradation of the surface has been observed over time.
- 2) The HTC for film boiling heat flux was found to be ~20X the HTC in nucleate boiling. This magnitude highlights the importance of operating with a safety margin.

Table 6

Mean absolute error (MAE) of existing correlations in predicting the current experimental data.

MAE [%]	Rohsenow [26]	Stephan and Abdelsalam [32]	Ribatski [30]	Cooper [29]	Nishikawa [31]	Li et al. [33]
SR1	23.8 %, $C_{sf} = 0.008$	16.7 %, $K_S = 70$	17.4 %	13 %, $K_c = 1500$	21 %, $K_S = 700$	200 %
SR2	46.8 %, $C_{sf} = 0.0043$	27.5 %, $K_S = 114$	28 %	23.8 %, $K_c = 1290$	31 %	53 %
SR3	39 %, $C_{sf} = 0.0037$	22.5 %, $K_S = 140$	22.6 %	17.8 %, $K_c = 1180$	26 %, $K_N = 700$	51 %
SR4	57 %, $C_{sf} = 0.0034$	23 %, $K_S = 160$	23.4 %	19.6 %, $K_c = 960$	29 %, $K_N = 700$	53.4 %

**Fig. 7.** Vertical orientation effect on the boiling curves of the smooth SR1 (a), and sandblasted SR3 (b) samples.

- Increasing the boiling surface area resulted in minimal impact on the average HTC, whilst higher HTC values have been observed with the vertical (90°) orientation. The CHF limit only showed small deviation with surface area in agreement with the literature of other dielectrics.
- Existing correlations to predict the pool boiling heat transfer and the effect of surface roughness have been compared to the experimental current data of Novec 649. The Ribatski and Jabardo [30] correlation gave the best prediction of surface roughness effect on pool boiling heat transfer of Novec 649, without the need of fitting the data.

Finally, the accurate experimental database of heat transfer pool boiling using Novec 649 is useful to validate other boiling heat transfer models and guide the selection of fluids for immersion cooling applications.

CRediT authorship contribution statement

Chiara Falsetti: Writing – review & editing, Writing – original draft, Project administration, Methodology, Investigation, Funding acquisition, Formal analysis, Data curation, Conceptualization. **Jason Chetwynd-Chatwin:** Resources, Project administration, Funding acquisition, Conceptualization. **Edmond J. Walsh:** Writing – review & editing, Methodology, Investigation, Funding acquisition, Formal analysis, Conceptualization.

Declaration of competing interest

The authors declare the following financial interests/personal relationships which may be considered as potential competing interests: EW and CF reports financial support was provided by Rolls-Royce plc. If there are other authors, they declare that they have no known competing financial interests or personal relationships that could have

appeared to influence the work reported in this paper.

Data availability

Data will be made available on request.

Acknowledgments

The authors gratefully acknowledge funding and technical support from Rolls-Royce plc and from the Ministry of Defence via the Defence Science and Technology Labs (DSTL), provided under contract DSTLX-1000152302.

References

- C. Falsetti, H. Jafarpourchekab, M. Magnini, N. Borhani, J. Thome, Two-phase operational maps, pressure drop, and heat transfer for flow boiling of R236fa in a micro-pin fin evaporator, *Int. J. Heat Mass Transf.* 107 (2017) 805–819.
- C. Falsetti, M. Magnini, J.R. Thome, Hydrodynamic and thermal analysis of a micro-pin fin evaporator for on-chip two-phase cooling of high density power micro-electronics, *Appl. Therm. Eng.* 130 (2018) 1425–1439.
- R.S. Bartle, K. Menon, E.J. Walsh, Pool boiling of resin-impregnated motor windings geometry, *Appl. Therm. Eng.* 130 (2018) 854–864.
- R.S. Bartle, E. Walsh, Bubble nucleators to enhance external pool boiling from the bottom row of a tube bundle, *Appl. Therm. Eng.* 178 (2020).
- R.S. Bartle, E. Walsh, Pool boiling of horizontal mini-tubes in unconfined and confined columns, *Int. J. Heat Mass Transf.* 145 (2019) 118733.
- A. Seshadri, K. Shirvan, Quenching heat transfer analysis of accident tolerant coated fuel cladding, *Nucl. Eng. Des.* 338 (2018) 5–15.
- R. Charlotte, F. Xuning, W. Gavin, L. Ruihe, W. Huaibin, R. Xinyu, L. Cheng, Z. Feng, N. Volker, P. Michael, P. Yatish, W. Yan, W. Hewu, O. Minggao, O. Gregory, W. Billy, Immersion cooling for lithium-ion batteries – a review, *J. Power Sources* 525 (2022) 0378–7753.
- V. Carey, *Liquid-Vapor Phase-Change Phenomena: An Introduction to the Thermophysics of Vaporization and Condensation Processes in Heat Transfer Equipment*, Taylor & Francis Group, New York, 2008.
- J. Collier, J. Thome, *Convective Boiling and Condensation*, Oxford Science Publications, 1994.

- [10] P. Birbarah, T. Gebrael, T. Foulkes, A. Stillwell, A. Moore, R. Pilawa-Podgurski, N. Miljkovic, Water immersion cooling of high power density electronics, *Int. J. Heat Mass Transf.* 147 (2020) 118918.
- [11] G. Liang, I. Mudawar, Review of pool boiling enhancement by surface modification, *Int. J. Heat Mass Transf.* 128 (2019) 892–933.
- [12] W. Li, R. Dai, M. Zeng, Q. Wang, Review of two types of surface modification on pool boiling enhancement: passive and active, *Renew. Sustain. Energy Rev.* 130 (109926) (2020).
- [13] Y. Song, C. Wang, D. Preston, G. Su, M.M. Rahman, H. Cha, B.P. Seong, J. Hiyun, M. Bucci, E. Wang, Enhancement of boiling with scalable sandblasted surfaces, *ACS Appl. Mater. Interfaces* 14 (2022) 9788–9794.
- [14] M. Može, V. Vajc, M. Zupancic, I. Golobic, Hydrophilic and hydrophobic nanostructured copper surfaces for efficient pool boiling heat transfer with water, water/butanol mixtures and Novec 649, *Nanomaterials* 11 (3216) (2021).
- [15] L. Lin, Y. Hu, M. Zu, Z. Su, K. Liu, C. Fan, J. H. Boiling heat transfer on the micro-nano structured surface fabricated by mechanical sandblasting/alkali-assisted oxidation, *Int. J. Heat Mass Transf.* 183 (122079) (2022).
- [16] A. Zou, S. Maroo, Critical height of micro/nano structures for pool boiling heat transfer enhancement, *Appl. Phys. Lett.* 103 (221602) (2013).
- [17] B. Jones, J. McHale, S. Garimella, The influence of surface roughness on nucleate pool boiling heat transfer, *ASME J. Heat Transf.* 131 (12) (2009).
- [18] E. Forrest, L.-W. Hu, J. Buongiorno, Pool boiling performance of Novec 649 engineered fluid, in: *ECI International Conference on Boiling Heat Transfer*, Florianopolis-SC-Brazil, 2009.
- [19] R. Kaniowski, R. Pastuszko, L. Nowakowski, Effect of geometrical parameters of open microchannel surfaces on pool boiling heat transfer, *EPJ Web Conf.* 143 (2017).
- [20] Z. Cao, Z. Zan Wu, B. Sundén, Heat transfer prediction and critical heat flux mechanism for pool boiling of NOVEC-649 on microporous copper surfaces, *Int. J. Heat Mass Transf.* 141 (2019) 818–834.
- [21] O. Ghaffari, F. Grenier, J.-F. Morissette, M. Bolduc, S. Jasmin, J. Sylvestre, Experimental Investigation of the effect of heat spreading on boiling of a dielectric liquid for immersion cooling of electronics, *J. Electron. Packag.* 143 (041103) (2021).
- [22] M. Shamsaiee, S. Holagh, M. Abdous, H. Saffari, Experimental investigation of surface finishing technique impact on subcooled flow boiling heat transfer enhancement: sandpapering and sandblasting, *Heat Mass Transf.* 58 (2022) 1785–1810.
- [23] S. Kline, F. McClintock, Describing uncertainties in single-sample experiments, *Mech. Eng.* 75 (1) (1953) 3–8.
- [24] Z. Wu, Z. Cao, B. Sundén, Saturated pool boiling heat transfer of acetone and HFE-7200 on modified surfaces by electrophoretic and electrochemical deposition, *Appl. Energy* 249 (2019) 286–299.
- [25] J.H. Lienhard, V.J.H. Lienhard, *A Heat Transfer Textbook*, Phlogiston Press, Cambridge, MA, 2020.
- [26] B. Mikic, W. Rohsenow, A new correlation of pool boiling data including the effect of heating surface characteristics, *J. Heat Transfer* 91 (1969) 245–250.
- [27] N. Zuber, *Hydrodynamic Aspects of Boiling Heat Transfer*, Doctoral Dissertation of University of California, 1959.
- [28] J. Kim, S. Jun, S. You, Effect of surface roughness on pool boiling heat transfer at a heated surface having moderate wettability, *Int. J. Heat Mass Transf.* 101 (2016) 992–1002.
- [29] M. Cooper, Saturation nucleate pool boiling - a simple correlation, in: *First UK National Conference on Heat Transfer*, University of Leeds, 1984.
- [30] G. Ribatski, J. Jabardo, Experimental study of nucleate boiling of halocarbon refrigerants on cylindrical surfaces, *Int. J. Heat Mass Transf.* 46 (2003) 4439–4451.
- [31] K. Nishikawa, Y. Fujita, H. Ohta, S. Hidaka, Effect of the surface roughness on the nucleate boiling heat transfer over the wide range of pressure, in: *Proceedings of the Seventh International Heat Transfer Conference*, München, Germany, 1982.
- [32] K. Stephan, M. Abdelsalam, Heat transfer correlations for natural convection boiling, *Int. J. Heat Mass Transf.* 23 (1980) 73–78.
- [33] Y.-Y. Li, Y.-J. Chen, Z.-H. Liu, A uniform correlation for predicting pool boiling heat transfer on plane surface with surface characteristics effect, *Int. J. Heat Mass Transf.* 77 (2014) 809–817.
- [34] K. Rainey, S. You, Effects of heater size and orientation on pool boiling heat transfer from microporous coated surfaces, *Int. J. Heat Mass Transf.* 44 (2001) 2589–2599.
- [35] M. Egbo, M.N.Y. Borumand, G. Hwang, Review: surface orientation effects on Pool-boiling with plain and enhanced surfaces, *Appl. Therm. Eng.* 204 (117927) (2022).
- [36] S. Jung, H. Kim, Effects of surface orientation on nucleate boiling heat transfer in a pool of water under atmospheric pressure, *Nucl. Eng. Des.* 305 (2016) 347–358.
- [37] A. Howard, I. Mudawar, Orientation effects on pool boiling critical heat flux (CHF) and modeling of CHF for near-vertical surfaces, *Int. J. Heat Mass Transf.* 42 (9) (1999) 1665–1688.